LIQUID-METAL-FED PULSED ELECTROMAGNETIC THRUSTERS FOR IN-SPACE PROPULSION*

T.E. Markusic
NASA Marshall Space Flight Center
Huntsville, AL

ABSTRACT

We describe three pulsed electromagnetic thruster concepts, which span four orders of magnitude in power processing capability (100 W to >100 kW), for in-space propulsion applications. The primary motivation for using a pulsed system is to is to enable high (instantaneous) power operation, which provides high acceleration efficiency, while using considerably less (continuous) power from the spacecraft power system. Unfortunately, conventional pulsed thrusters require failure-prone electrical switches and gas-puff valves. The series of thrusters described here directly address this problem, through the use of liquid metal propellant, by either eliminating both components or providing less taxing operational requirements, thus yielding a path toward both efficient and reliable pulsed electromagnetic thrusters. The emphasis of this paper is to conceptually describe each of the thruster concepts; however, initial test results with gallium propellant in one thruster geometry are presented. These tests reveal that a greater understanding of gallium material compatibility, contamination, and wetting behavior will be necessary before a completely functional thruster can be developed. Initial experimental results aimed at providing insight into these issues are presented.

INTRODUCTION

MOTIVATION

Electromagnetic accelerators provide the clearest path toward viable high-power electric propulsion systems, because of their inherently high thrust density and high thrust efficiency (at high power). Yet, extensive research has shown that the thrust efficiency of these devices (e.g., the magnetoplasmadynamic (MPD) thruster) is prohibitively low (η_t<50%) at input power levels lower than $\mathcal{O}(1)$ MW[1]. The efficiency can be increased at lower power levels by augmenting the system with a strong applied magnetic field; however, the substantial mass of the magnet leads to a markedly higher thruster α. Even with the addition of an applied field, only Russian thrusters operating with lithium propellant have demonstrated η_t>40%.

The high efficiency of high-power electromagnetic acceleration can, in principle, be accessed at substantially lower continuous power levels by using a *pulsed* electromagnetic accelerator. This is accomplished by capacitively storing energy at relatively low power, and then releasing it in an intense, high-power burst. A heuristic example: a pulsed electromagnetic accelerator could store 10 kJ of energy, in a capacitor, over a time period of 1 sec (10 kW input power), and then release the energy in a current pulse of approximately 10 µsec duration, resulting in an instantaneous thruster power of $\mathcal{O}(1)$ GW. Operating the thruster at 10 Hz rep-rate would require 100 kW continuous input power; however, the physics governing the acceleration process would occur at GW power levels, and hence yield high thrust efficiency. While the benefits of pulsed electromagnetic acceleration are evident, the development of a practical system has proven to be elusive — and not for lack of trying. Institutionally diverse research efforts during the 1960s produced repetitively pulsed thrusters with I_{sp}>6000 sec and corresponding η_t>50%. However, two persistent issues have prevented high-power pulsed electromagnetic thrusters from being seriously considered for flight applications: the unavailability of reliable, efficient pulsed power circuity and pulsed propellant delivery systems.

The process of storing and releasing electrical energy requires a high current electrical switch. To date, no switch has been developed which can provide *both* the required current ($\mathcal{O}(10^5)$ A) and lifetime ($\mathcal{O}(10^9)$ pulses). Similarly, high speed gas puff valves, which are used to meter propellant into the thruster prior to each current pulse, have not demonstrated the required lifetime. As failure of either one of these components during a spaceflight mission would lead to a complete loss of the thruster, the conventional high-power pulsed thruster designs possess intrinsic liabilities that will limit their application. While these realities may appear to paint a rather bleak picture, our intention here is to emphasize that the development of new pulsed electromagnetic accelerators can only be justified if the effort addresses both the electrical switching and propellant valving issues head-on. Accordingly, our aim through the present program is to implement new ideas that directly address these problems, which will make pulsed electromagnetic accelerators viable propulsion devices.

---

*This effort was performed under sponsorship of the NASA MSFC CDDF and NASA TIPS programs.

PROJECT OVERVIEW

NASA Marshall Space Flight Center's Propulsion Research Center (PRC) is presently investigating three electric propulsion concepts which utilize liquid metal propellants. These thrusters are: the Liquid-Fed Pulsed Plasma Thruster (LFPPT), the Pulsed Lorentz Force Accelerator (PLFA), and the Two-Stage Pulsed Plasma Thruster (TSPPT). All of the devices are designed to utilize pulsed electromagnetic acceleration to produce thrust. Pulsed electromagnetic accelerators are highly scalable with input power level. We are developing three thruster concepts that span power processing capabilities from sub-kilowatt to hundreds of kilowatts. We are particularly interested in metallic propellants because their high electrical conductivity and low vapor pressure may be exploited to enable plasma thruster designs that eliminate failure-prone components and increase efficiency. Metallic propellants provide additional benefits such as small, lightweight propellant tanks, due to their high mass density (as compared to high-pressure gas fed systems). We are presently investigating gallium and lithium propellants.

Research into new thruster concepts is only warranted if detailed analysis shows that the new thruster may provide either performance, reliability, or system integration benefits (preferably all) above existing thrusters. Also, there must exist a space flight mission for which the new thruster's performance parameters are well matched. The series of thrusters that we are presently proposing aim to provide significantly higher specific impulse, over all input power levels, than current flight-qualified thrusters. High specific impulse thrusters are a compulsory technology for large-scale robotic or piloted outer planetary exploration, and hence validate this line of research. In Fig. 1 we illustrate performance parameters for a variety of thrusters (thrust efficiency is given in parentheses). The black points represent very well characterized, flight qualified thrusters. The red points represent experimental thrusters, for which performance data may be limited. While this figure is not intended to be comprehensive, an important conclusion can be gleaned from the figure; there exists a need for high thrust density, high specific impulse thrusters -- over the entire range of current and projected power levels. The performance goals for our proposed thrusters are indicated by the red stars in the figure. If successfully developed, each of these thrusters will provide new high specific impulse capabilities within their respective power regimes.

The LFPPT is designed for lower power missions (sub-kW). A highly efficient, lower specific impulse (~1000 sec) version of the LFPPT could be used as an attitude control thruster, whereas a high specific impulse version (~3500 sec) could be a viable alternative Radioisotope Electric Propulsion (REP) thruster. The PLFA is designed to operate in the 10 kW power regime, and hence provide an alternative Solar Electric Propulsion (SEP) thruster. The PLFA could offer higher specific impulse (~4500 sec) and lower system mass than current ion thrusters. The TSPPT is engineered to provide high specific impulse (~7500 sec) propulsion at very high power levels associated with Nuclear Electric Propulsion (NEP). Thrusters such as the TSPPT will be needed to support Project Prometheus objectives.

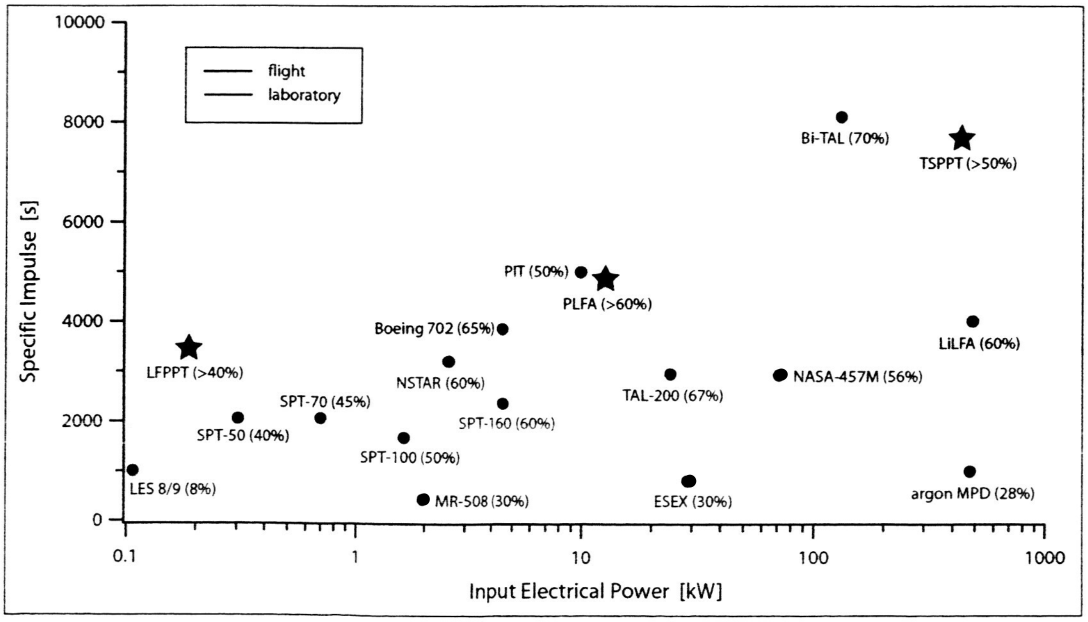

Figure 1. Performance goals for MSFC liquid-metal-fed pulsed electromagnetic thrusters (addti-tional, representative thrusters included for comparison).

Below we provide more detailed descriptions of each thruster concept. But first we describe our efforts to develop a liquid metal feed system, which is a common component of all three thrusters.

LIQUID METAL FEED SYSTEM (LMFS)

Metallic propellants have been used in almost all major categories of electric propulsion devices. Ion, MPD, and Hall thrusters have demonstrated high performance with metallic propellants (using mercury, lithium and bismuth, respectively). Laboratory testing of any of these devices requires a propellant feed system that accurately meters propellant at a specified flow rate. Flight experiments will have the added demands of high reliability and low system mass. We have developed a compact, robust liquid metal feed system (LMFS) that does not require pressurized gas, valves, or other moving parts. The system provides repeatable, precise, continuous mass flow to thrusters, which is essential for accurate evaluation of thruster performance. Also, the simplicity of the design may make it a candidate for implementation on spacecraft.

The high electrical conductivity of metallic propellants can be exploited to enable the use of non-mechanical propellant pressurization and flow-rate sensing. A schematic illustration of the LMFS is shown in Fig. 2a. Solid metal is melted in a heated reservoir (the temperature ranges from approximately 30 C° for gallium to 300 C° for bismuth). Gravity causes the liquid to flow into the propellant feed line, and "prime" the MHD pump. When electrical current is applied to the MHD pump, the fluid in the feed line rises above its equilibrium level and flows into the thruster. The desired propellant flow rate is established by varying the current through the MHD pump. The mass flow rate can be correlated with pump current through calibration, or measured directly by continuously monitoring the fluid height in the reservoir.

A photograph of a prototype MHD pump is shown in Fig. 2b. Liquid metal enters the pump through a tube fitting and electrically shorts two silver electrodes, that are on opposing sides of the pump. Two samarium-cobalt permanent magnets are located on the top and bottom of the pump, providing a strong magnetic field (~0.2 Tesla) through the liquid metal, transverse to the two electrodes. The pump is shrouded in a soft iron yoke, which both confines and strengthens the magnetic field inside the pump. When voltage is applied between the two electrodes, current flows through the liquid metal, transverse to the applied magnetic field, imparting a Lorentz force on the fluid, which causes it to flow in the direction of **JXB**. For example, using the pump pictured below and 1/4" feed lines, pumping gallium (approximately) 3 cm above its equilibrium height requires an applied voltage of about 0.1 V, and results in a current of approximately 10 A. Lithium, which is considerably less dense than gallium, will require less current, whereas bismuth will require sustantially more. The total pump power input is generally on the order of a few watts. We have also developed a simple, yet accurate mass flow rate sensor. Two very thin, highly resistive stainless steel wires are immersed in the reservoir. A 100 mA precision current source drives current down one wire, through the liquid metal, and back up the other wire. The voltage between the wires is monitored using a 24-bit A/D converter. As the fluid level recedes during pumping, the voltage between the wires increases, because the length of the wire above the fluid (and hence the resistance) increases. For a typical reservoir loaded with approximately 100 g of propellant, mass changes of 10-100 μg are measurable.

We are developing feed systems to handle gallium and lithium propellants. Gallium has the benefit of ease

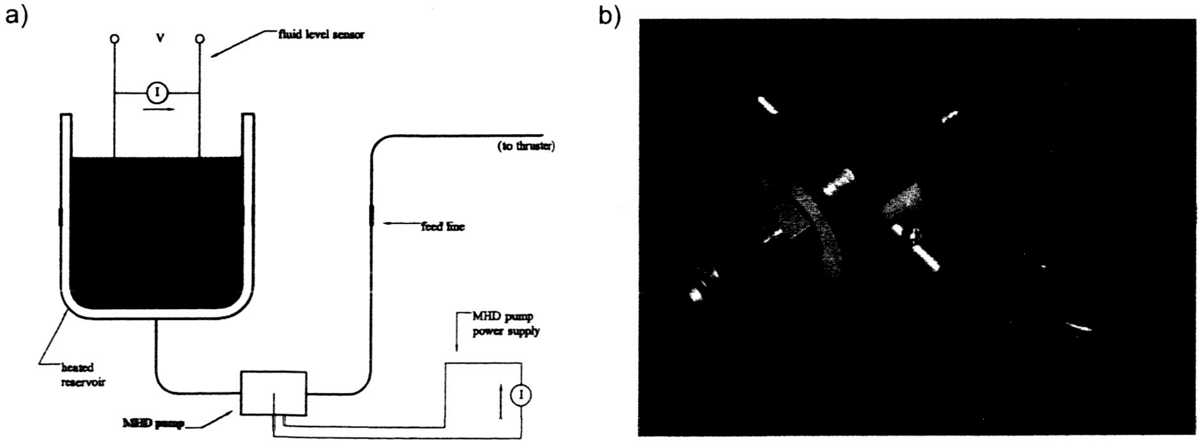

Figure 2. a) Schematic illustration of LMFS components, b) photograph of prototype MHD pump.

of handling (low melting temperature and toxicity), and is presently being implemented in our pulsed plasma thruster program. Lithium, while being more difficult to handle, has low atomic mass and low first ionization potential, and has been shown to enable high efficiency, high specific impulse operation in MPD thrusters[2].

Propellant contamination (especially oxygen) can be detrimental to thruster component lifetime. We have constructed a hermetically sealed, stainless steel glove box for loading propellant into the LMFS. The glove box uses a purifier system to monitor and reduce oxygen and moisture levels to less than 1 ppm. The enclosure also provides a safe environment for handling hazardous propellants, such as lithium.

LIQUID-FED PULSED PLASMA THRUSTER (LFPPT)

The Pulsed Plasma Thruster (PPT) was one of the earliest electric propulsion devices to be developed, originating from the so-called Marshall gun used in fusion research during the 1950s[3]. The PPT was actively developed through 1960s, but eventually fell out of favor as more promising concepts, such as the MPD thruster, began to emerge. Below we describe why the PPT failed to realize its potential, and describe a new type of PPT, the Liquid-Fed PPT (LFPPT), which eliminates the deficiencies found in earlier PPT designs, and shows promise as a viable alternative low-power electric propulsion device.

Two classifications of PPTs are well developed; they are distinguished by the corresponding form of propellant used: gas-fed (GFPPT) or ablative propellant (APPT). The gas-fed variety has the advantages of a "clean" exhaust plume and high specific impulse. The ablative version of the PPT uses a solid propellant, such as Teflon, to provide other advantages such as mechanical simplicity, compactness, and overall ease of system integration, but with modest performance (typical values are I_{sp}=1000 sec and η_t=8%). Existing high-power GFPPT designs have weak features, most notably, low thrust efficiency and lifetime (reliability), that have prevented them from reaching the high level of technology readiness and application enjoyed by APPTs.

Poor dynamic, propellant utilization and electrical efficiencies are the primary detractors from efficient GFPPT operation[4]. Propellant sweeping using a propagating current sheet is a fundamentally inefficient process; GFPPT dynamic efficiency can be as low as 50%. Reliable gas valves capable of cycling in less than 100 µs are not available; hence, GFPPTs continue to flow (and waste) propellant after the electrical circuit has discharged. GFPPTs require high voltage, low capacitance energy storage (to generate satisfactory current sheets). The external circuit is usually poorly impedance matched to the load (the thruster), and low electrical efficiency results. GFPPTs require high speed gas valves and high current electrical switches. Neither of these components have demonstrated technology readiness to withstand the billions of cycles that would be required for many spaceflight missions. These components present a considerable liability for a flight GFPPT system, as a failure of either one would result in the loss of the thruster.

The LFPPT, which utilizes liquid metal propellant, circumvents many of the negative GFPPT issues through a design that requires neither a gas valve nor an electrical switch, and should, in principle, be a very efficient and reliable thruster. The principle of operation is as follows. Low melting temperature liquid metal propellant (such as gallium, which is liquid at room temperature) is stored in an un-pressurized reservoir. The propellant is delivered from the reservoir to the thruster using an MHD pump. Precise control of the metal mass flow rate is accomplished by simply adjusting the current to the pump. The MHD pump has no moving parts – emphasizing an attractive feature of using a conductive propellant. The main thruster components are two electrodes and a low voltage ($\mathcal{O}$(100 V)), high capacitance ($\mathcal{O}$(1) mF), low inductance pulse capacitor bank (see Fig. 3a). Near the breach, the electrodes are separated by a small gap ($\mathcal{O}$(0.1) mm), after which they flare to ($\mathcal{O}$(1) cm) separation at the exit. After the capacitor bank is charged, liquid metal is pumped through a small hole in the anode -- forming a droplet. Eventually the droplet grows large enough in size to bridge the anode-cathode gap, thus "shorting" the system. Current flow commences through the droplet, causing rapid heating, vaporization, and ionization. The high electrical current (($\mathcal{O}$(10) kA) and associated self-magnetic field, exerts an axially directed Lorentz force, which accelerates the metal plasma along the electrodes. The plasma is ejected at high speed (($\mathcal{O}$(10) km/sec), and thrust is derived. After ejection, the circuit is once again open and the process is repeated at a frequency of $\mathcal{O}$(10) Hz.

Let us return to the PPT efficiency issues alluded to above, and contrast the LFPPT operation with conventional GFPPTs. The LFPPT should deliver high dynamic efficiency because the propellant is loaded in the optimal "slug" configuration, as opposed to the "snowplow" loading in conventional GFPPTs. Loading all of the propellant at the breach of the thruster allows for continuous acceleration and, hence, high dynamic efficiency. The propellant loading scheme should also provide high propellant utilization, since (snowplow) current sheet permeability is avoided; also, the so-called "late-time vaporization" found in APPTs should not occur, since the propellant source is not directly exposed to the current sheet during the acceleration process. Finally, the low-voltage operation of the

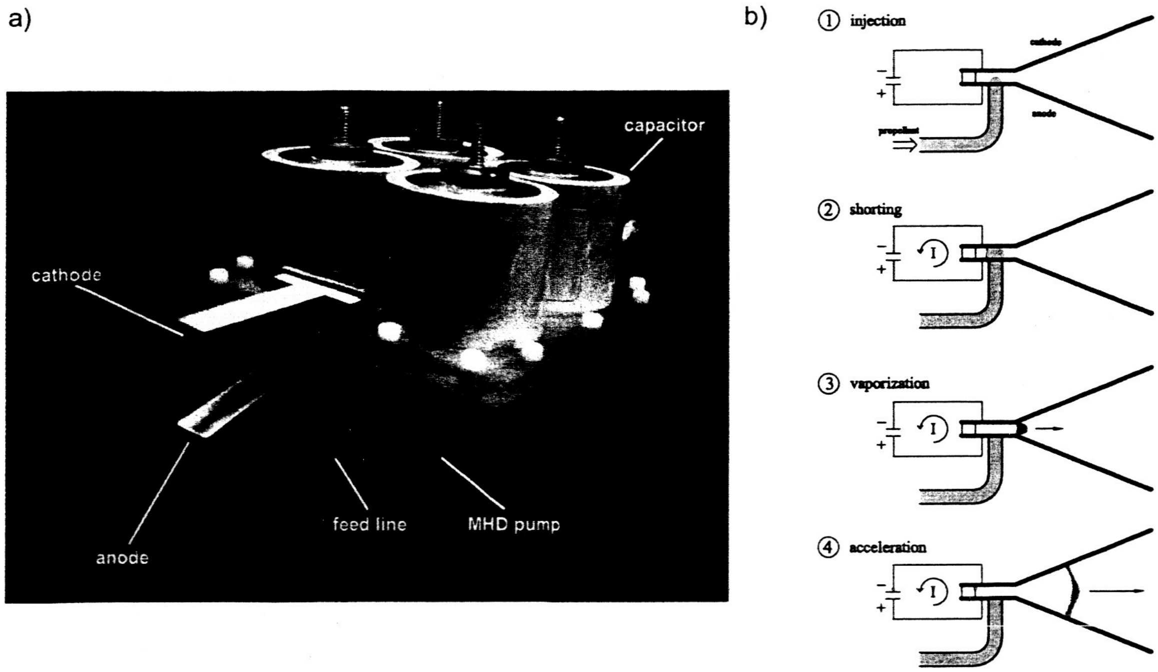

Figure 3. a) Photograph of LFPPT-2, b) LFPPT principle of operation.

LFPPT allows for better impedance matching between the (typically high impedance) source (capacitor bank) and (typically low impedance) load (acceleration channel) and, hence, higher electrical efficiency. Conventional GFPPTs must operate at high voltage in order to break down the (neutral) gas and form a viable, continuous current sheet (skin effect), whereas the LFPPT automatically forms a narrow current channel, due to the highly localized injection of conductive propellant. So, for a given initial energy, the LFPPT can operate at lower voltage ($\mathcal{O}(10)^2$ V versus $\mathcal{O}(10)^3$ V) and higher bank capacitance ($\mathcal{O}(1)$ mF versus $\mathcal{O}(10)$ μF). Since the source impedance scales as $(1/C)^{1/2}$, the LFPPT source impedance can be made considerably lower than is possible in a GFPPT, and hence will provide for more efficient transfer of energy to the load. Lastly, the lower operating voltage capability may couple more favorably (versus ion thrusters, which operate at >1 kV) to high efficiency radioisotope power generators, making the LFPPT a competitive REP technology.

The latest version of the LFPPT (LFPPT-2) is shown above in Fig. 3a. The thruster uses gallium propellant, and its physical dimensions are approximately 6" X 6" (top view). It is powered by four CSI 800 V, 150 μF polypropylene dielectric metallized film capacitors, providing up to 200 J per pulse. The capacitors were custom-designed to allow for coaxial projection of the top electrode, yielding very low inductance (<10 nH). The thruster's overall parasitic inductance, including the transmission lines, is estimated to be less than 10 nH. The electrodes are brass, with 3/8" diameter tungsten inserts at the breach (where initiation occurs), The propellant reservoir (500 g capacity) and MHD pump are located under the capacitors. Initial LFPPT-2 tests results are described in the Results and Discussion section of this paper.

PULSED LORENTZ FORCE ACCELERATOR (PLFA)

The Pulsed Lorentz Force Accelerator (PLFA) is an electric propulsion concept that aims to provide high specific impulse and thrust efficiency over a broad range of input power levels (0.1-10 kW). The PLFA combines design elements of the Lithium Lorentz Force Accelerator (LiLFA), quasi-steady MPD thrusters, and pulsed plasma thrusters. The PLFA incorporates new ideas which directly address problems that have plagued earlier pulsed MPD thrusters. Most notably, the PLFA design requires no high-speed gas valves and uses a porous, liquid-metal-weeping electrode to reduce electrode erosion. A schematic illustration of the components of the complete PLFA system is shown in Fig. 4a. These are analogous to those found in a conventional quasi-steady MPD thruster, the principal difference being the propellant feed system, which relies on the ablation of *liquid metal* propellant rather than a gas-feed system. The pulsed-power system, which uses a pulse transformer and an SCR switch, is also somewhat unique. The PLFA discharge chamber (see Fig. 4b) has the typical MPD coaxial electrode geometry, but with certain novel features: a porous frontal section of the cathode, through which liquid propellant is delivered; a metal baffle which provides shielding of the breech insulator from ultraviolet radiation and lithium back streaming; and an array of igniter plugs, which may be needed to trigger each discharge. The PLFA has a mechanically simple, robust design. The liquid-metal feed system requires no mechanical valves or moving parts, thus eliminating the failure-prone high speed valves found in gas-fed systems. The PLFA propellant tank and feed lines are unpressurized, which provides a reliability advantage over the high pressure xenon propellant storage used in ion thrusters. The propellant injection scheme will also mitigate electrode erosion. Since both the current conduction path and the propellant source are the molten metal on the anode surface, we are, in essence, feeding a liquid metal anode into the thruster, and using the electrode erosion products as the propellant. Rather than being a detrimental effect, electrode erosion is an essential facet of the PLFA operation. The integrity of the underlying electrode material is maintained, and long lifetime can be achieved.

The sequence of events in a single PLFA discharge cycle are as follows. Liquid lithium is pumped from a heated (~200 C°) reservoir into the thruster cathode using an MHD pump. The frontal section of the cathode is made of porous metal (e.g., sintered tungsten), which allows the lithium to "weep" through, coating the outside of the electrode with a thin layer of liquid lithium. At a prescribed time, a bank of SCRs is triggered, allowing the pulse-forming network (PFN) (~125 J) to discharge through a pulse transformer. The pulse transformer is impedance matched to the thruster to provide efficient, non-ringing transfer of energy to the thruster. Upon closure of the SCRs, an igniter circuit is simultaneously fired inside the thruster to provide an initial inter-electrode conducting medium; the secondary side of the pulse transformer is energized, and an arc discharge commences inside the thruster discharge chamber. The arc attachment at the cathode causes the liquid lithium to vaporize and ionize in the inter-electrode

a)

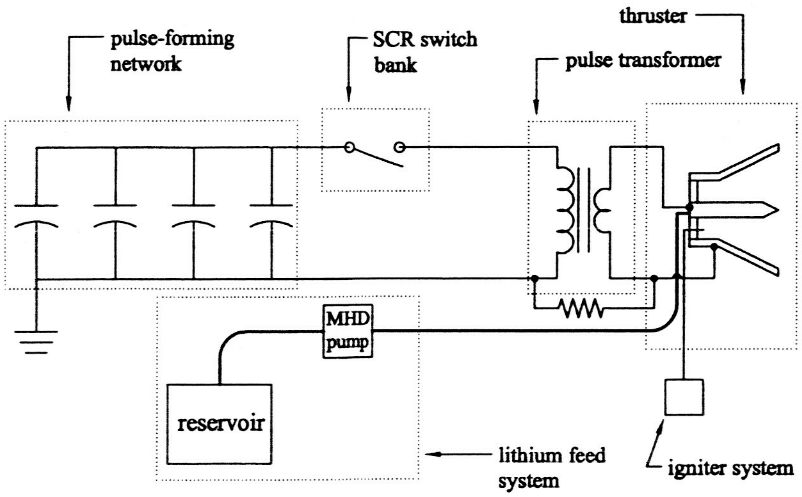

b)

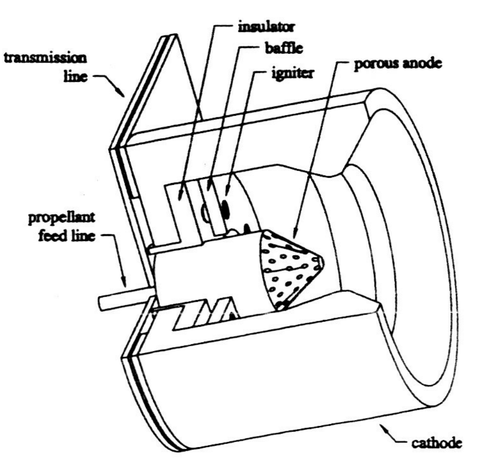

c)

Thruster	NSTAR	PLFA
Type	Ion	MPD
I_{sp} [s]	3127	4800
η_t [%]	60	60
P_{max} [kW]	2.3	12.5
T_{max} [mN]	92.7	365
T/P_{max} [mN/kW]	37	29
T/A [N/m^2]	1.3	50
α [kg/kW]	3.6	1.8

Figure 4. a) Schematic illustration of PLFA components, b) schematic illustration of PLFA discharge chamber, c) PLFA performance goals and comparison with NSTAR ion thruster.

region of the thruster, where it is accelerated. Thrust is primarily derived from the electromagnetic acceleration of the propellant, under the action of the Lorentz force. The thruster is repetitively pulsed at up to 100 Hz to accommodate power levels of up to 12.5 kW.

We have performed a preliminary analysis of the performance potential of the PLFA for solar-electric propulsion (SEP). The design power point for this thruster was 12.5 kW, but it is expected that a thruster designed to operate at sub-killowatt power levels would deliver similar performance. The table in Fig. 4c lists the results of that analysis (data for a typical ion thruster are included, for comparison). The difference in the physical mechanism by which power supply energy is coupled to the plasma (magnetic field versus electric field) gives rise to the most striking difference in the performance parameters between the PLFA and ion thrusters -- thrust density, T/A (thrust per unit area). The PLFA will have more than an order-of-magnitude higher thrust density than a typical ion thruster and, consequently, will be physically smaller and lighter (for a given power level). Also, the PLFA will be able to maintain relatively constant performance (both I_{sp} and η_t) over a wide range of input power levels. This is accomplished by maintaining constant discharge energy while varying the duty cycle to accommodate variations in available bus-power. This has significant benefits in relation to missions which call for a variation in input power (due to, for example, motion away from the Sun). Unlike the PLFA, Ion thruster performance can be strongly affected by input power level; the NSTAR thruster efficiency drops from approximately 60% at peak power to 40% at 0.5 kW.

TWO-STAGE PULSED PLASMA THRUSTER (TSPPT)

Pulsed plasma thrusters may have unique capabilities to satisfy the propulsion needs for missions that require high specific impulse, high thrust efficiency, and high thrust density, in the 100-500 kW power regime. The motivation of the Two-Stage Pulsed Plasma Thruster (TSPPT) project is to develop a high-power (~500 kW), high specific impulse (~7500 sec), highly efficient (>50%) thruster for use as primary propulsion in a high power nuclear electric propulsion system. High-energy PPTs have already been experimentally shown to be capable of accelerating current sheets to speeds greater than 150 km/s (corresponding to a specific impulse above 15,000 sec). Another study demonstrated high-energy PPT operation at greater than 60% thrust efficiency. These experiments prove that there are no fundamental physical limitations that will prevent us from attaining our stated design goals. The TSPPT project aims to provide the high performance observed in earlier PPTs, but with design enhancements that eliminate all moving parts and high-current electrical switches and thus dramatically improve system reliability.

The components of the TSPPT are schematically illustrated in Fig. 5a. The first stage (labeled "injector assembly") operates in the same manner as the LFPPT; the injector vaporizes, ionizes, and ejects a dense, thermal plasma -- in this case into the main (second stage) discharge cavity. Whereas the first stage operates at $\mathcal{O}(100)$ J, the second stage discharges $\mathcal{O}(10)$ kJ of capacitively stored energy to accelerate the effluent from the first stage to a speed on the order of 100 km/s. The conceptual evolution of the second stage current sheet is depicted in Fig. 5c. The second stage electrode configuration, which has essentially a hybrid z-pinch/coaxial geometry, uses a truncated inner electrode (cathode) to induce a ``virtual cathode" along the centerline of the accelerator. The goal is to maximize the acceleration channel inductance gradient and, hence, maximize the force on the current sheet. The current sheet will form near the back of the accelerator. The Lorentz force will drive it around the end of the cathode, pinching the plasma at the center, in a manner similar to a dense plasma-focus device. Provided that current continues to be driven by the capacitor, the anode current sheet attachment will continue to propagate axially, and the cathode column will be extruded, forming a ``virtual" center electrode. Since this type of current configuration is known to be MHD unstable, our research will seek to determine if appreciable acceleration can be realized before the current is disrupted.

We have constructed a prototype thruster (see Fig. 5b), TSPPT-1, to experimentally to investigate current sheet evolution in the TSPPT geometry. The thruster uses 4 17.5 μF Maxwell capacitors, and is capable of operating at up to 50 kJ per pulse. Later thrusters will operate at up to 10 Hz, providing power processing capability up to 500 kW. We have performed both 1-D "circuit" and 2-D MHD numerical modelling of the TSPPT-1. The 1-D model predicts a peak current of approximately 1 mega-ampere, and a terminal current sheet speed of approximately 100 km/s. The 2-D simulations were carried out using MACH2[5]; these simulations indicate that the current structures envisioned in Fig. 5c will indeed form in a manner very similar to the conjectured, conceptual evolution.

RESULTS AND DISCUSSION

To date, we have only carried out experiments on the LMFS and the LFPPT. The results of those experiments are discussed below.

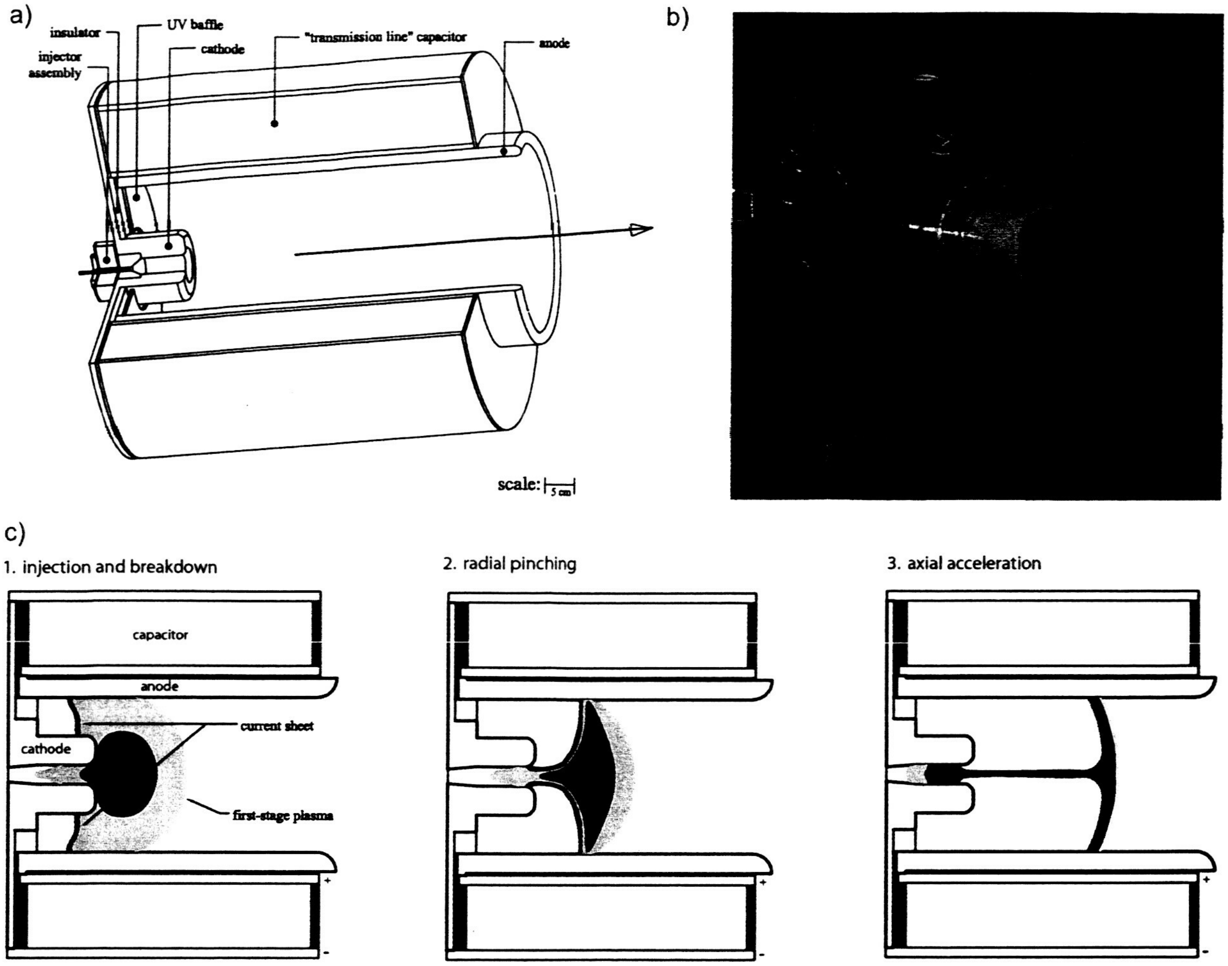

Figure 5. a) Schematic illustration of TSPPT components, b) photograph of TSPPT-1, c) conceptual evolution of current sheet in TSPPT second stage.

<u>LMFS RESULTS</u>

An experimental apparatus was assembled to demonstrate that an MHD pump could be used to meter propellant at flow rates of propulsive interest. More specifically, we were interested in demonstrating controlled flow at rates consistent with the requirements for our liquid-metal-fed pulsed plasma thrusters: ~100 μg/sec for the LFPPT up to ~1 mg/sec for the TSPPT. A photograph of the experimental apparatus is shown in Fig. 6a. Gallium was loaded into the heated (~30 C°) reservoir; since the fluid level of the gallium in the reservoir was above the height of the feed line exit, flow immediately initiated. The exiting gallium was captured in a cup, which was located on a precision balance, and the total mass change as a function of time was recorded, as shown in Fig. 6b. Similarly, the experiment was repeated, but with 10 A MHD pump current and the polarity set to retard ("negative" bias) the flow. It is clear from the figure that the pump was effective in providing a constant force to slow the flow from 1.4 mg/sec to 600 μg/sec. When the pump current was set to 20 A, the flow was stopped completely. While this "retrograde" pumping configuration will not necessarily be used in feeding propellant to thrusters, this simple experiment does demonstrate the capability of this type of MHD pump to control the flow of liquid metal propellants.

<u>LFPPT RESULTS</u>

The LFPPT-2 thruster shown in Fig. 3a was tested with gallium propellant. Note that the propellant reservoir is located below the feed line exit (anode orifice) in the LFPPT-2 so that the MHD pump must be operated with "forward" bias – to lift the propellant in the feed line above the reservoir level. Operation in this configuration produced

a) b)

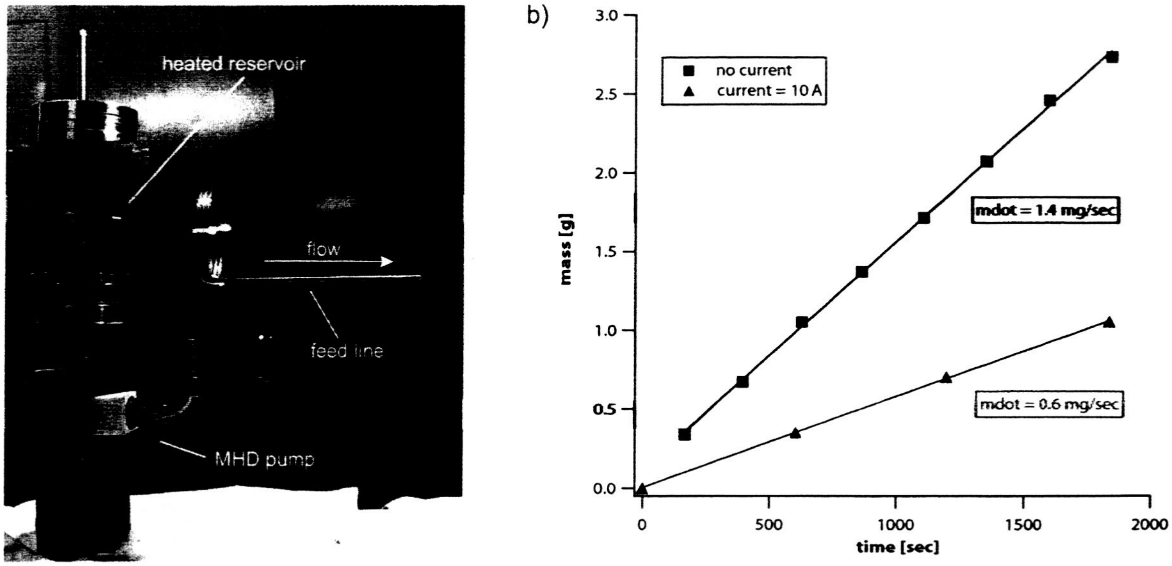

Figure 6. a) Photograph of LMFS test apparatus, b) mass flow data using gallium propellant.

unexpected complications, as will be discussed further below.

With the capacitor voltage set to 600 V (monitored using a Tektronix Model P6015 high-voltage probe), current was applied to the MHD pump to initiate propellant flow. However, no flow was induced at current levels (~10 A) expected to provide the requisite flow rate (~100 μg/sec). Incrementally increasing the pump current eventually led to propellant flow, but at current levels substantially higher than projected (~35 A) and with immediate negative consequences, as shown in Fig. 7. The series of video images shows that between frames 1 and 2, as desired, liquid gallium shorts the inter-electrode gap and plasma is produced; however, after several rapid bursts similar in appearance to frame 2, the gallium completely "floods" the gap (frame 3), permanently short circuiting the capacitors, which prevents subsequent re-charging. The cause of this undesirable sequence of events is the fact that substantially more force (pump current) is required to start the flow of propellant than is required to maintain steady flow; once flow is initiated in the LFPPT-2, the feed line rapidly becomes over-pressurized, causing copious amounts of propellant to flow through the anode orifice, and subsequent flooding.

Despite the fact that we were only able to fire several shots in a given experimental run, we were able to acquire information about the circuit behavior. Figure 8 shows two typical current waveforms (derived from differentiating the voltage waveform). The two waveforms (from different runs) overlap well -- indicating repeatable shot-to-shot behavior. The peak current is approximately 180 kA, which is remarkably high for a discharge initiated at only 600 V. The high current likely stems from two sources -- one good and one bad. On the positive side, the current waveform reveals that the effort to lower the source impedance was successful. This is confirmed by the rapid current rise rate ($\mathcal{O}(10)^{11}$ A/sec), which is consistent with the estimated <10 nH parasitic inductance. On the down side, the high peak current and substantial current reversal suggest that the current channel is not rapidly propagating away from the

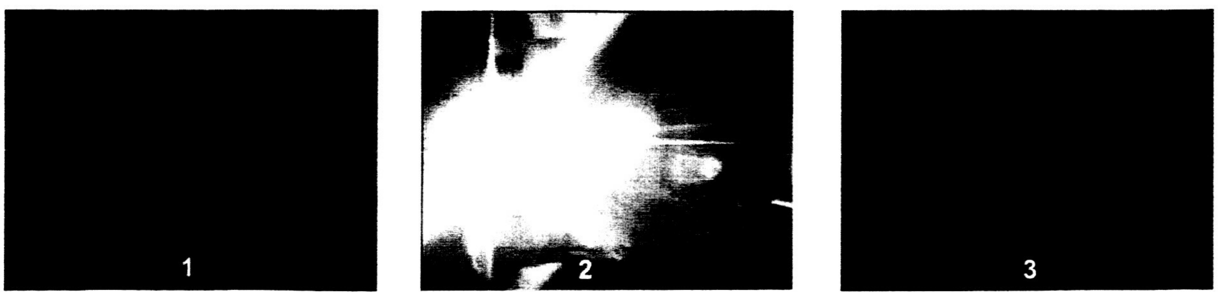

Figure 7. Series of video images showing LFPPT-2: 1) before initiation, 2) firing, 3) flooded (note gallium bridging electrodes).

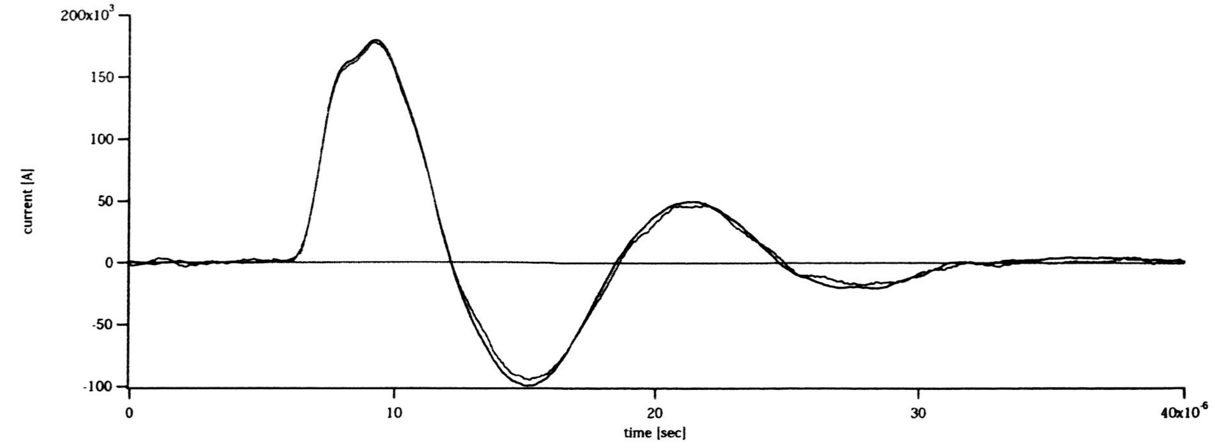

Figure 8. Two (typical) current waveforms for LFPPT-2 operation at 600 V.

breach of the thruster, that is, energy is not being efficiently deposited in (thrust-bearing) plasma acceleration. Also, some modest loss of total capacitance (~1%) was observed, indicating that the high current levels were damaging the (self-healing) metallized film capacitors.

CONTAMINATION, WETTING, AND MATERIAL COMPATIBILITY STUDY

The need to understand and gain better control of the liquid metal flow start-up process has forced us to consider more deeply the influence of propellant contamination, capillarity, wetting phenomena, and material compatibility. We constructed a dedicated experiment to address the two latter issues, to answer the following questions: at what temperature does gallium wet various materials, and how does gallium interact with these materials at elevated temperatures? The apparatus is shown in Fig. 9a. It consisted of a heated aluminum block with four holes, in which four material samples (1/2" diameter disks) were press-fitted: alloy 360 brass, alloy 145 copper, alloy 304 stainless steel, and "chatter-free" tungsten (90% W, 6% Ni, 4% Cu). Two thermocouples were mounted on opposing sides of the aluminum block, to allow continuous monitoring of the block temperature. A single drop of gallium was placed on each sample (a drop was placed in the center of the aluminum block as well), and the apparatus was placed in a vacuum chamber, which was then evacuated to ~5 mTorr. The block temperature was increased from room temperature to 400 C° over a period of about four hours. Visible changes in the geometry of the droplets, and the corresponding block temperature, were noted during the heating process.

a) b)

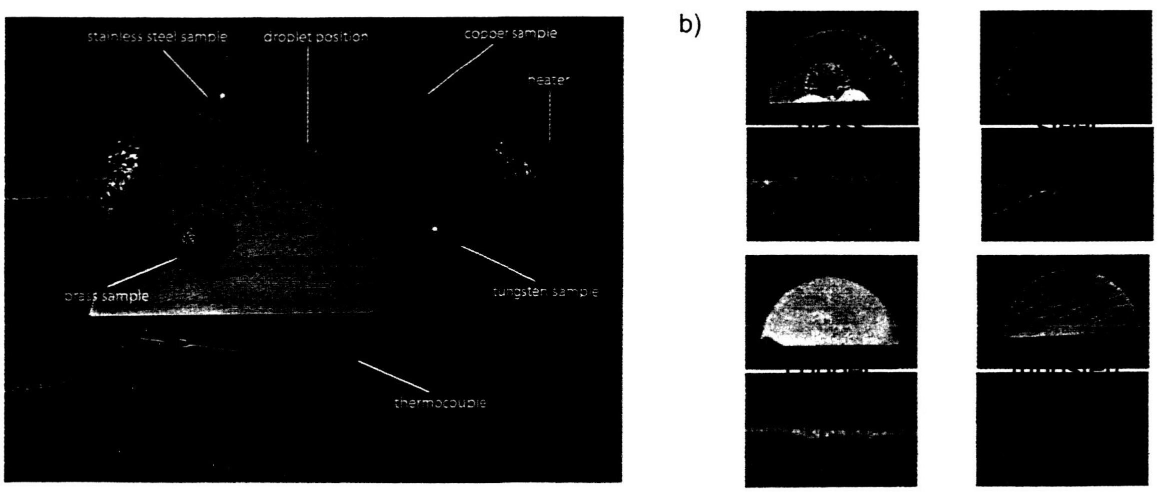

Figure 9. a) Wetting and compatiblity study apparatus (photographed after test), b) top view and cross section of metal samples, after test.

Several interesting and relevant phenomena were observed during the experiment. First, it was notable that as the gallium droplets were initially placed on the metal samples, they did not take on an ellipsoidal shape, as would be expected but, rather, they maintained the shape of a teardrop. The droplets maintained this teardrop shape up to approximately 350 C°, suggesting that the initial shape was not due to freezing at the surface, but some form of surface contamination that formed a rigid structure to support the non-equilibrium teardrop geometry. Except for the collapsing of the teardrop shape to an ellipsoidal shape, no visible changes were observed on the stainless steel or tungsten samples, during the entire heating process (i.e., no wetting was observed). Similarly, the brass sample showed little variation, except for a slight reduction in the gallium-brass surface contact angle above approximately 350 C°. The droplet in the center of the aluminum block showed the most dramatic variation. At approximately 140 C° the gallium droplet disappeared altogether, as if it were absorbed by the aluminum. Subsequent heating resulted in a "dimple" in the aluminum, around which formed a widely dispersed "halo" (see Fig. 9a). At approximately 375 C°, the gallium was observed to wet the copper sample. Subsequent examination of the metal samples revealed additional interesting information. Figure 9b shows photographs of the post-test samples (which were cut in half to reveal inner detail). The side views of both the copper and brass samples reveal penetration of gallium into the bulk material of the sample. Evidently gallium alloys, or is absorbed into copper and brass in the temperature range of our experiment. While the stainless steel and tungsten samples show blemishes from the presence of gallium on the surface, penetration of gallium into the material is not observed in the side views of the samples.

In relation to thrusters, several useful insights can be gleaned from the wetting and compatibility study. First, when gallium is exposed to air, it rapidly forms a surface film that is mechanically strong. This may explain why unexpectedly high currents were required to induce flow in LFPPT-2; a large force may have been required to initially rupture the film at fluid surface -- inside the feed line. Second, gallium does not appear to wet typical materials at temperatures of interest (<100 C°) for application in PPTs. Lastly, aluminum, copper and brass were shown to be unsuitable electrode materials in regions where hot liquid gallium is expected to exist, as rapid degradation (pitting) of the material would be expected. All of these conclusions, however, are based on observations of gallium that was contaminated by exposure to air. Pure gallium may behave quite differently; a similar study in a controlled environment will be necessary to confirm these findings. We also expect to find additional relevant studies in the literature.

FUTURE WORK

Our effort to develop liquid-metal-fed pulsed electromagnetic thrusters is clearly at a very early stage, with most of the ideas still at an unproven, conceptual level. Our immediate plans for the project are as follows. The LMFS requires more quantitative calibration experiments in order to characterize the accuracy of the flow rate control. Also, tests with more reactive propellants, such as lithium, need to be carried out. In the LFPPT project, the problem of the initial propellant surge needs to be remedied, possibly by using a pulsed pumping scheme. Also, the injection geometry will need to be modified in order to promote more rapid acceleration of the initial current channel. The PLFA project will remain on hold until a funding source is secured. First tests of the TSPPT will take place very soon. Gaseous propellant injection may be used initially, to simplify operation during the initial runs. A (translating) array of magnetic field probes has been constructed to immediately allow for interrogation of the current sheet evolution -- for comparison with the modelling effort.

ACKNOWLEDGEMENTS

We thank Drs. Stephen Rodgers, Charles Schafer, and Jeffrey Sheehy for encouragement and support. We gratefully acknowledge the invaluable contributions of the PRC In-Space Propulsion Group technical support staff: Doug Davenport, Doug Galloway, Mike Lee, Tommy Reid, Jeff Richeson, and Dexter Strong. Dr. Jason Cassibry of UAH and Dan Franco of General Dynamics have heavily contributed to the MACH2 modeling. Elements of the PLFA design originated through discussions with Profs. Rod Burton of UIUC and Dennis Keefer of UTSI.

REFERENCES

1. J.K. Ziemer and E.Y. Choueiri. ***Quasi-steady magnetoplasmadynamic thruster performance database, Journal of Propulsion and Power***, 17(4):520-529, (Sep 2001).
2. V.P. Ageyev, V.P. Ostrovsky, and V.A. Petrosov. ***High-current stationary plasma accelerator of high power***. In 23rd International Electric Propulsion Conference, 1993. IEPC-93-117.
3. J. Marshal. ***Performance of a hydromagnetic plasma gun***. The Physics of Fluids, 3(1):134-135, (Jan-Feb 1960).
4. J.K. Ziemer and E.Y. Choueiri. ***Scaling laws for electromagnetic pulsed plasma thrusters***, Plasma Sources Science and Technology, 10(3):395-405, (Aug 2001).
5. R.E. Peterkin Jr. and M.H. Frese. ***MACH: A Reference Manual -- First Edition***. Air Force Research Laboratory (1998).